Electronic Supplementary Material (ESI) for Polymer Chemistry.

Facile construction of fluorescent polymeric aggregates with various morphologies by self-assembly of supramolecular amphiphilic graft copolymers

Xiaofan Ji,[a] Yang Li,[b] Hu Wang,[a] Run Zhao,[a] Guping Tang,[b] and Feihe Huang*[a]

[a]*State Key Laboratory of Chemical Engineering, Center for Chemistry of High-Performance & Novel Materials, Department of Chemistry, Zhejiang University, Hangzhou 310027, P. R. China*

Fax and Tel: +86-571-8795-3189; Email: fhuang@zju.edu.cn

[b]*Department of Chemistry, Institute of Chemical Biology and Pharmaceutical Chemistry, Zhejiang University, Hangzhou 310027, P. R. China*

Electronic Supplementary Information

1. Materials and methods

Compound **4**[S1] and polymer **2**[S2] were prepared according to literature procedures. Solvents were either employed as purchased or dried according to procedures described in the literature. ^{1}H NMR spectra were collected on a Bruker Advance DMX-400 spectrometer with internal standard TMS. Molecular weight distributions were measured on a conventional gel permeation chromatography (GPC) system equipped with a Waters 1525 Isocratic HPLC pump, a Waters 2414 refractive index detector, and a set of Waters Styragel columns (HR1, HR2 and HR4, 7.8 mm × 300 mm). GPC measurements were carried out at 35 °C using DMF as the solvent with a flow rate of 1.0 mL/min. The system was calibrated with linear polystyrene standards. Dynamic light scattering (DLS) was carried out on a Malvern Nanosizer S instrument at room temperature. SEM investigations were carried out on a JEOL 6390LV instrument. Transmission electron microscopy investigations were carried out on a HITACHI HT-7700 instrument. Atomic force microscopy investigations were carried out on a MultiMode 8 instrument. Fluorescent confocal images were recorded on a Zeiss LSM 710 confocal fluorescence microscopy. The fluorescence spectra were recorded on a Perkin Elmer LS55 fluorescence spectrophotometer. The critical aggregation concentration values of the polymer aggregates were determined on a DDS-307 instrument. MTT assay was applied to evaluate the cytotoxicity of the samples in HepG2 cells.[S3] HepG2 cells were seeded in the 96-well plates and cultured at 37 °C in a 5% CO_2 humidified atmosphere for 18 h. The aggregate dispersions with various concentrations were added to each well, and the cells were subjected to MTT assay after being incubated for another 24 h. The absorbance of the solution was measured on a Bio-Rad model 550 microplate reader at 570 nm. Cell viability (%) was equal to $(A_{sample}/A_{control}) \times 100$, where A_{sample} and $A_{control}$ denote the absorbances of the sample well and control well, respectively. Experiments were performed in quadruplicate. *In vitro* intracellular trafficking: the intracellular trafficking of samples was examined by confocal microscopy using HepG2 cells. The cells were seeded on 24-well plates at 2×10^4 cells/well in 800 μL of RPMI-1640 medium containing 10% FBS and was allowed to grow for 18 h. The medium was replaced by 400 μL of serum-free culture media containing solutions of samples (80 μg/mL). After 4 h, the cells were rinsed and fixed with fresh 4% paraformaldehyde, and then the cells were treated with 5.0 μg/mL WGA in PBS for 1 h. The confocal images were acquired on a confocal scanning laser microscope (CLSM, Radiance 2100, Bio-Rad).

*2. Synthesis of polymers **3** and **1***

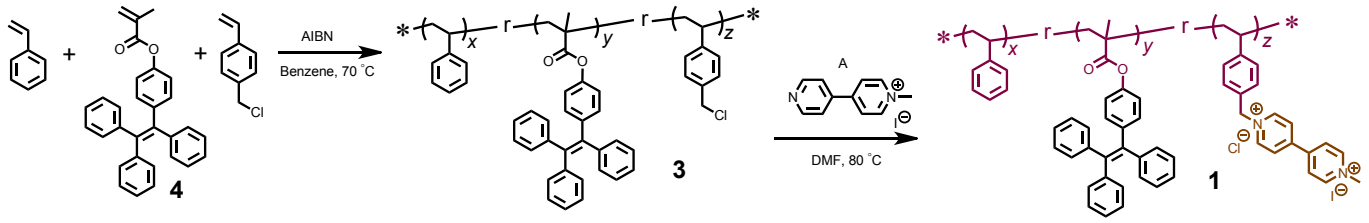

Scheme S1. Synthetic route to polymer **1**.

Polymer **3** was prepared from styrene, compound **4**, and 4-vinylbenzyl chloride by free radical polymerization. A mixture of styrene (1.20 mL, 10.5 mmol), compound **4** (4.36 g, 10.5 mmol), and 4-vinylbenzyl chloride (1.50 mL, 10.5 mmol) in 30 mL of benzene was stirred at room temperature. A stream of argon (Ar) was bubbled through for 30 min. In one portion was added 34.4 mg (0.209 mmol) of azobisisobutyronitrile (AIBN) and the mixture was stirred for 10 min, sealed with a rubber septum and heated to 70 °C for 24 h. The polymerization was quenched by rapid freezing in liquid nitrogen and the solvent was removed under vacuum. The crude product was dissolved in 2 mL of $CHCl_3$ and precipitated into 200 mL of methanol. The precipitated solid was collected by vacuum filtration. This process was repeated three times and the collected polymer was dried in vacuo (2.13 g, 30%). ^{1}H NMR (400 MHz, $CDCl_3$, 298 K) δ (ppm): 7.24–6.80 (m, 50H, *Ar*), 6.78–6.28 (m, 20H, *Ar*), 4.52 (m, 2H, Ar-CH_2-), 2.13–1.68 (m, mainchain, 11H), 1.51–1.11 (m, mainchain, 41H), 0.94–0.82 (m, 9H, CH_3).

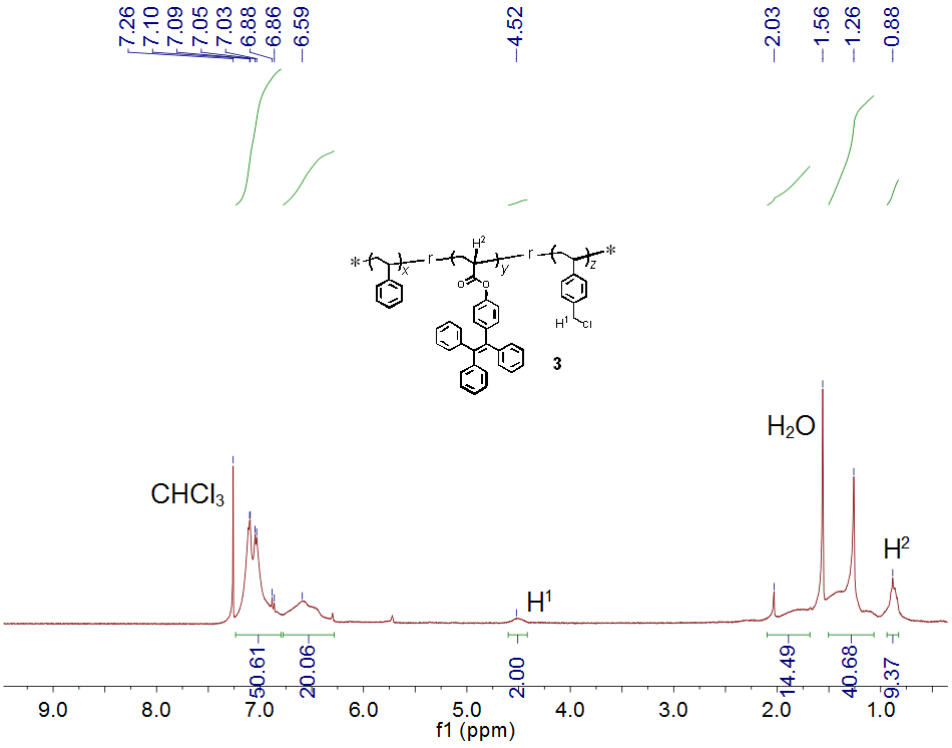

Fig. S1. ^{1}H NMR spectrum (400 MHz, $CDCl_3$, 298 K) of polymer **3**.

The ratio of *y*/*z* was (9.37/3)/(2/2), namely 3.12/1, as calculated based on the integrations of the peaks of H_2 and H_1, and *x*/*z* was 1.45/1 as calculated based on the integrations of peaks of benzene protons. Therefore, the ratio of *x*/*y*/*z* was 1.45/3.12/1 for polymer **3**.

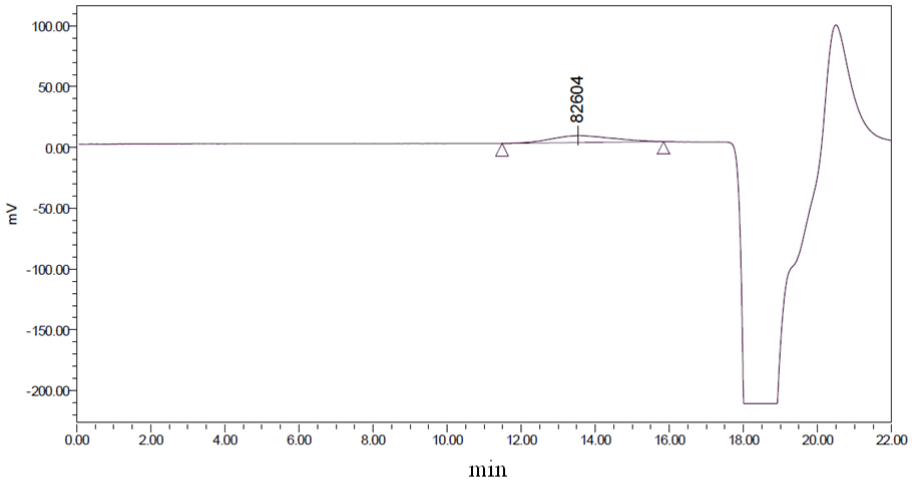

M_n	M_w	M_p	M_z	PDI
49495	97783	82604	176040	1.68

Fig. S2. GPC analysis of polymer **3** using conventional calculations, with polystyrene as the standard and DMF as the solvent.

According to M_n and the ratio of *x*/*y*/*z*, it can be calculated that the values of *x*, *y*, and *z* were 45, 96 and 31, respectively.

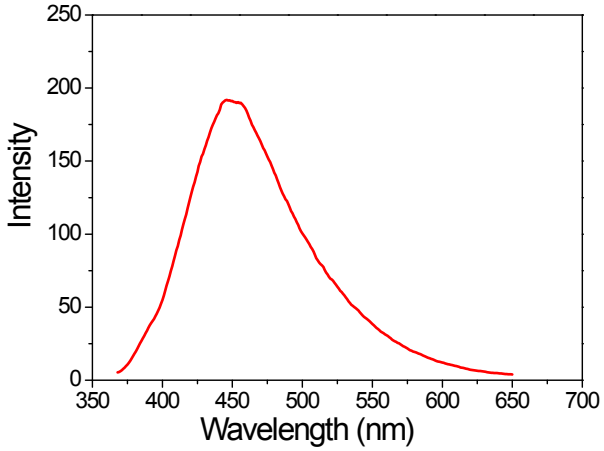

Fig. S3. Fluorescence spectrum of polymer **3** (1.71×10^{-5} M) in $CHCl_3$, λ_{ex} = 332 nm.

A mixture of polymer **3** (1.00 g, 0.0200 mmol) and compound **A**[S4] (1.79 g, 6.00 mmol) in DMF (50 mL) was stirred at 80 °C overnight. The solvent was evaporated and the residue was dissloved in 2.00 mL of chloroform. Then the solution was dropped into cold methanol (100 mL) and the precipitate was collected by filtration; the process was repeated. The solid was dried overnight in a vacuum to give a brown power (0.961 g, 82%). The ^{1}H NMR spectrum of polymer **1** is shown in Fig. S4. ^{1}H NMR (400 MHz, $CDCl_3$, 298 K) δ (ppm): 9.32 (m, 4H, pyridine), 8.87 (m, 4H, pyridine), 7.24–6.81 (m, 50H, *Ar*), 6.80–6.27 (m, 18H, *Ar*), 4.59 (m, 5H, Ar-CH_2-pyridine and methyl), 2.17–1.10 (m, 57H, main chain), 1.00–0.77 (m, 9H, CH_3).

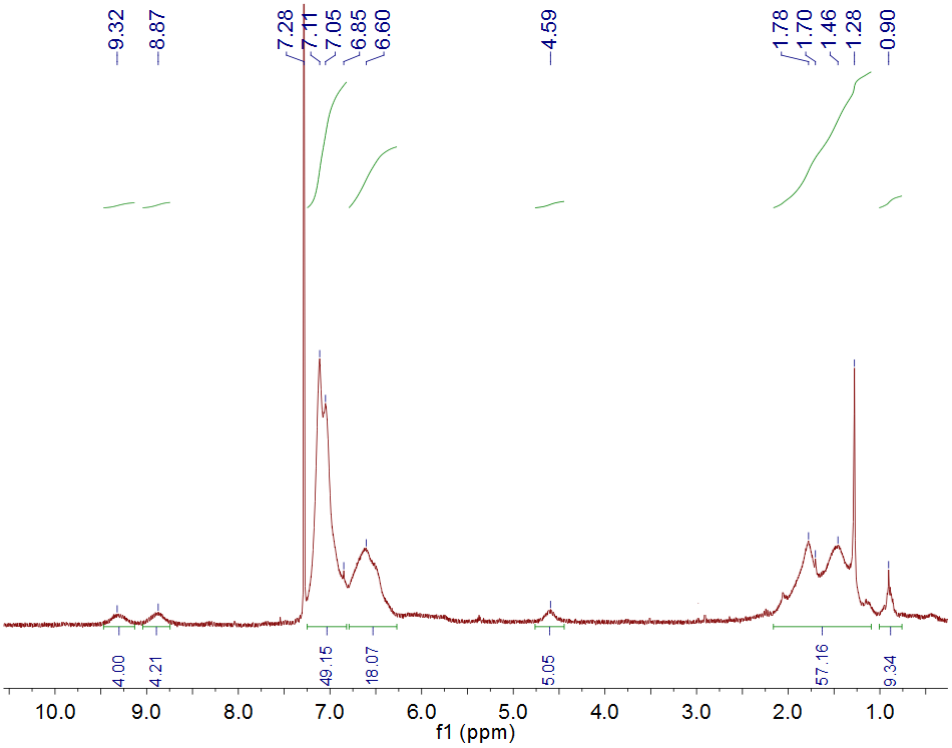

Fig. S4. ^{1}H NMR spectrum (400 MHz, $CDCl_3$, 298 K) of polymer **1**.

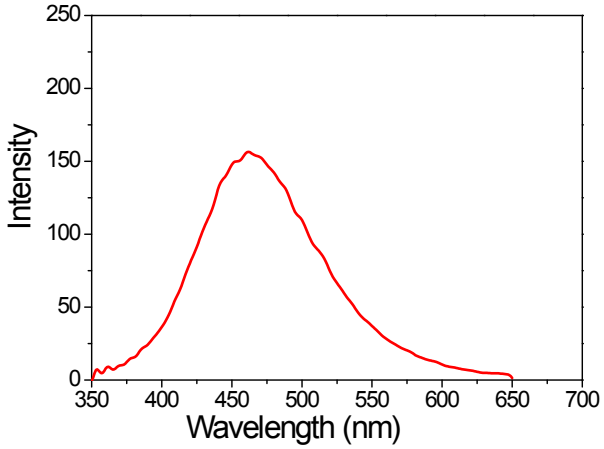

Fig. S5. Fluorescence spectrum of polymer **1** (1.71×10^{-5} M) in $CHCl_3$, λ_{ex} = 332 nm.

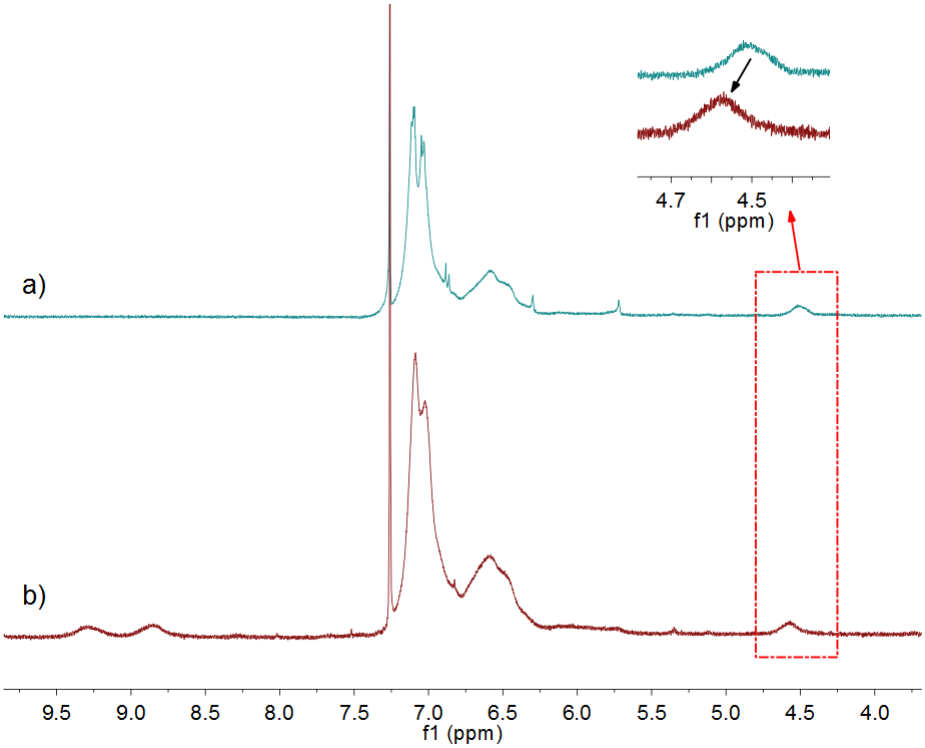

Fig. S6. Partial ^{1}H NMR spectra (400 MHz, $CDCl_3$, 293 K): (a) **3** (1.71×10^{-5} M); (b) **1** (1.71×10^{-5} M); Insert: enlarged picture of peaks from 4.3 to 4.8 ppm.

It can be seen that the peak corresponding to the methylene protons in the -Ar-CH_2-pyridinium part shifts downfield compared with that for the case of the -Ar-CH_2Cl group, indicating the conversion from polymer **3** to polymer **1**. The M_n value of polymer **3** is 4.95×10^4, so the M_n value of polymer **1** was calculated to be 5.85×10^4.

*3. ^1H NMR spectra of polymer **2** and compound **4***

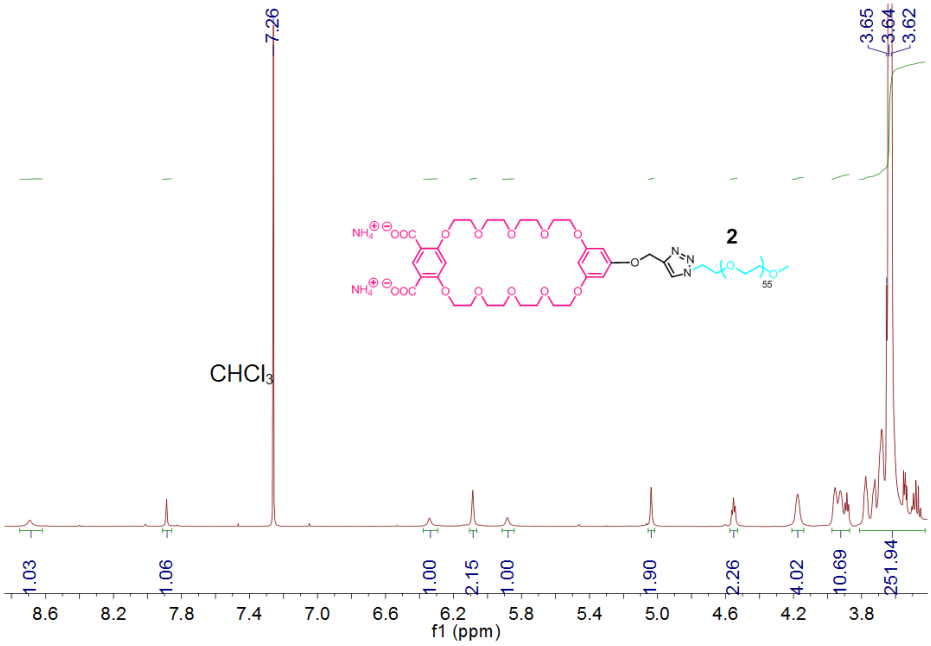

Fig. S7. ^{1}H NMR spectrum (400 MHz, $CDCl_3$, 298 K) of **2** (M_n = 3900).

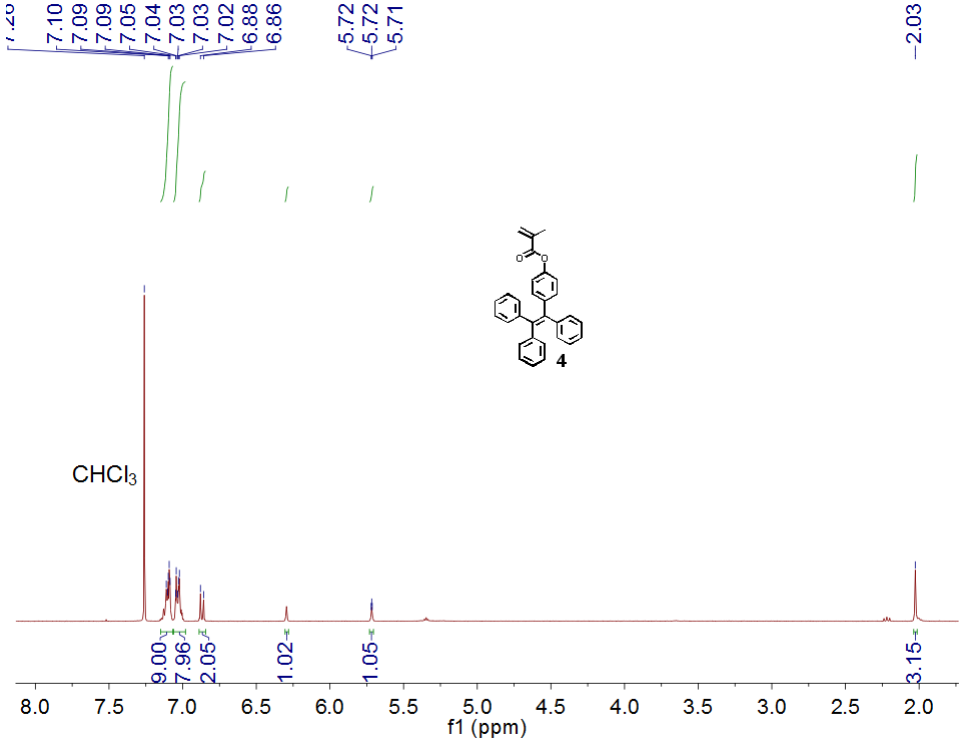

Fig. S8. ^{1}H NMR spectrum (400 MHz, $CDCl_3$, 298 K) of **4**.

*4. DLS results for solutions of **1** and **2** with different molar ratios*

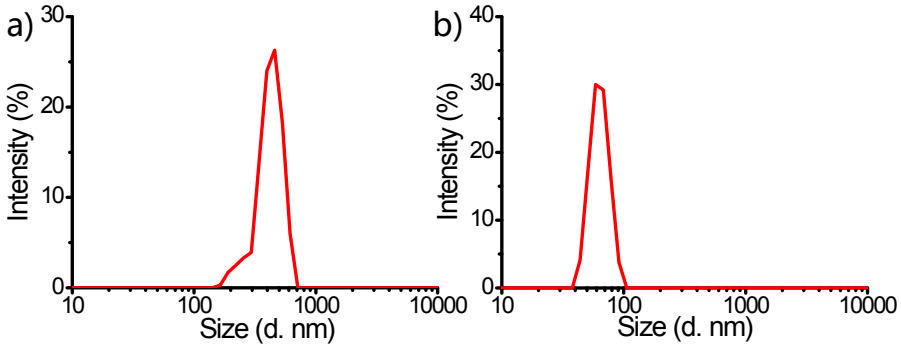

Fig. S9. DLS results: a) a water solution of 1.71×10^{-5} M (5.30×10^{-4} M in paraquat units) **1** and 3.41×10^{-4} M **2**; b) a water solution of 1.71×10^{-5} M (5.30×10^{-4} M in paraquat units) **1** and 5.12×10^{-4} M **2**.

5. Fluorescence spectra of the polymeric aggregates in aqueous solution

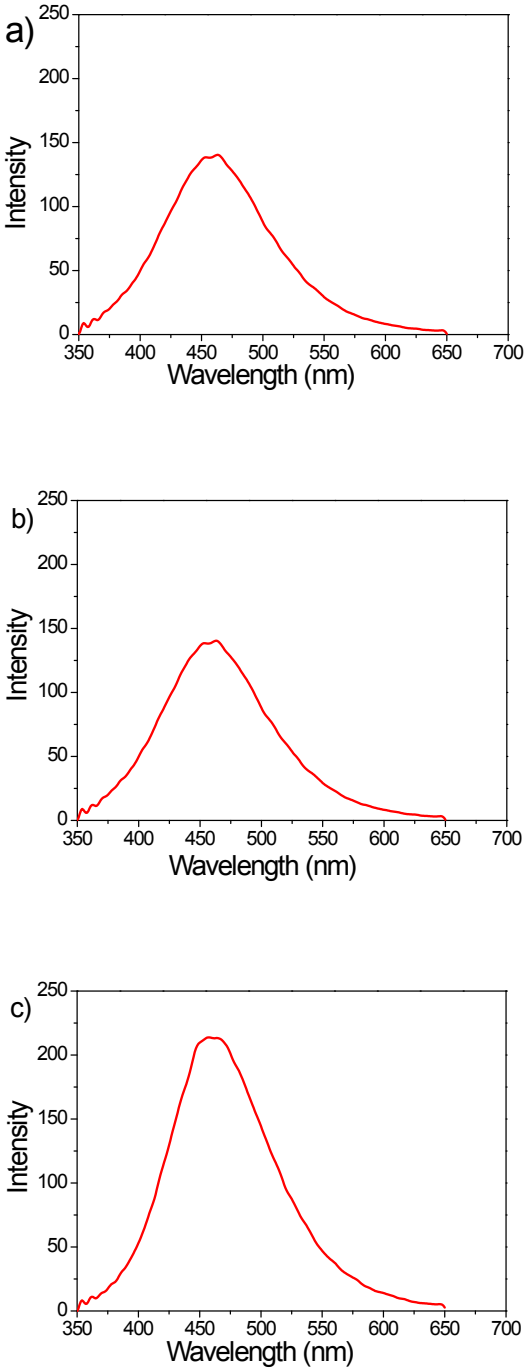

Fig. S10. Fluorescence spectra of the polymeric aggregates in aqueous solution with different polymer concentrations: a) 1.71×10^{-5} M (5.30×10^{-4} M in paraquat units) **1** and 1.71×10^{-4} M **2**; b) 1.71×10^{-5} M (5.30×10^{-4} M in paraquat units) **1** and 3.41×10^{-4} M **2**; c) 1.71×10^{-5} M (5.30×10^{-4} M in paraquat units) **1** and 5.12×10^{-4} M **2**, λ_{ex} = 332 nm.

*6. Critical aggregation concentrations of mixtures of polymers **1** and **2** determined by conductivity measurements*

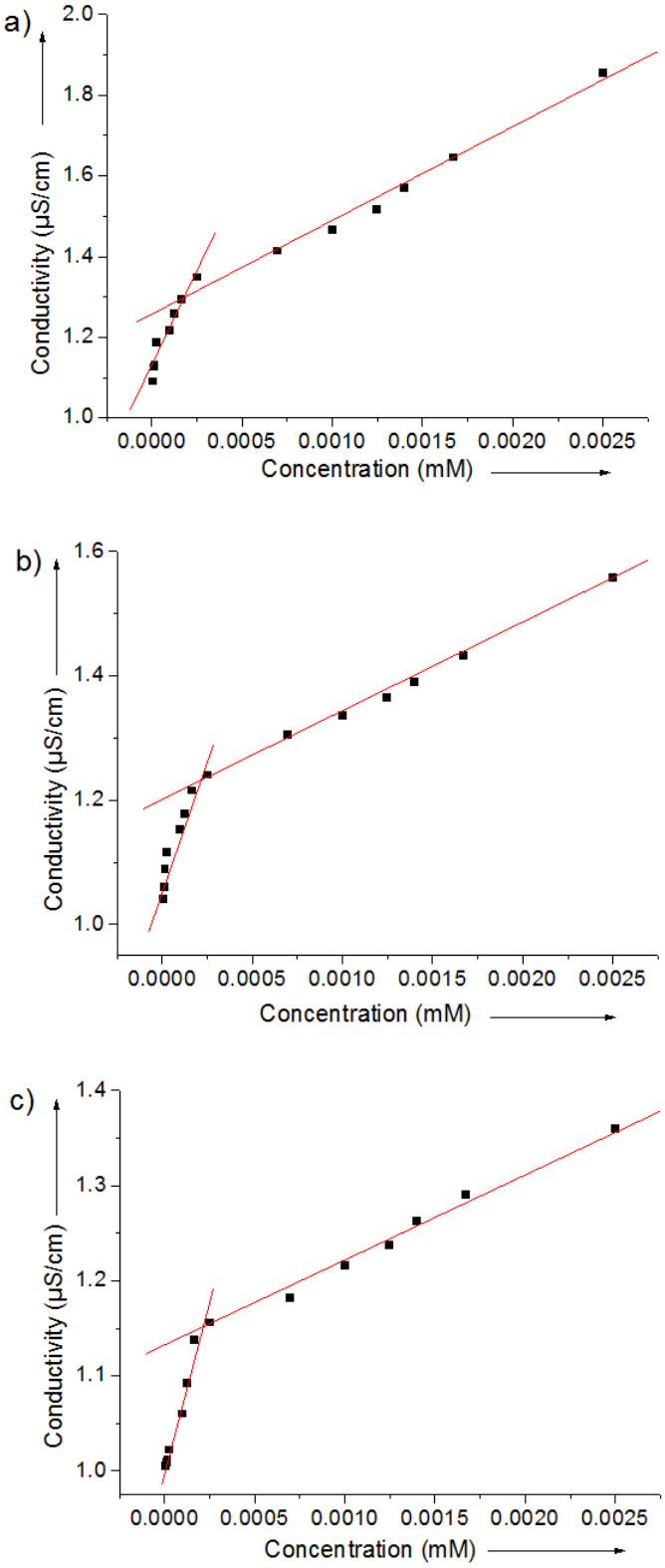

Fig. S11. Conductivity (κ) versus the concentration of polymer **1** for mixtures of polymers **1** and **2** with different mixing molar ratios of polymers **1** and **2**: a) 1 : 10; b) 1 : 20; c) 1 : 30.

*7. Cytotoxicity of polymers **1** and **2**, and their mixtures against HepG2 cells*

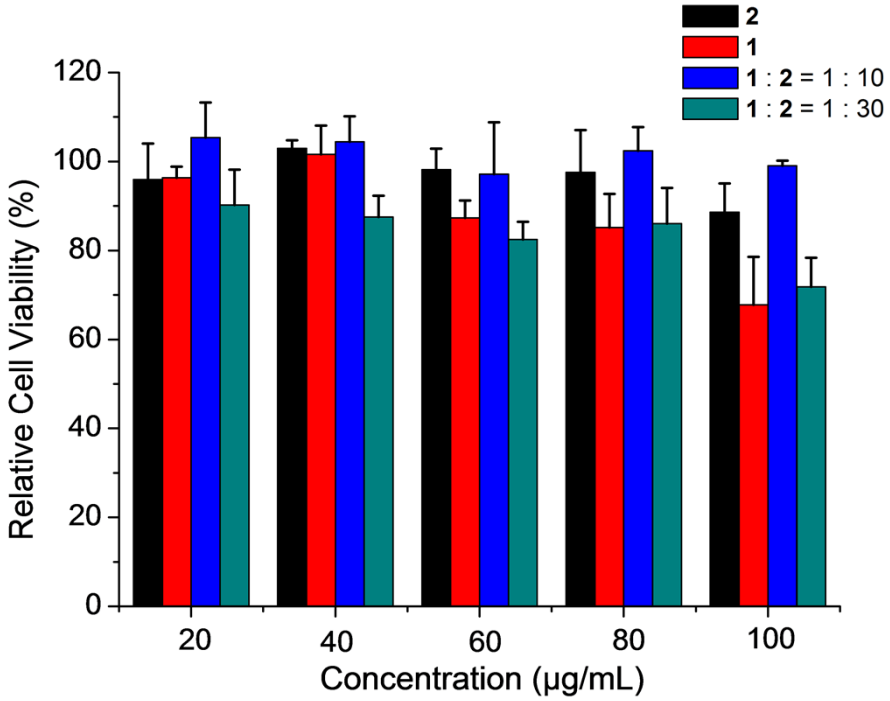

Fig. S12. Cytotoxicity of polymer **2**, polymer **1**, and two mixtures of polymers **1** and **2** with different molar ratios against HepG2 cells.

The cytotoxicity of **1**, **2**, and the polymeric aggregates were investigated in HepG2 cells (human liver hepatocellular carcinoma cell line) using a 3-(4',5'-dimethylthiazol-2'-yl)-2,5-diphenyl tetrazolium bromide (MTT) assay.[S3] That cells maintained high viabilities indicated low cytotoxicity of **1**, **2** and the polymer aggregates according to the results from Fig. S12.

8. AFM results of the polymeric vesicles

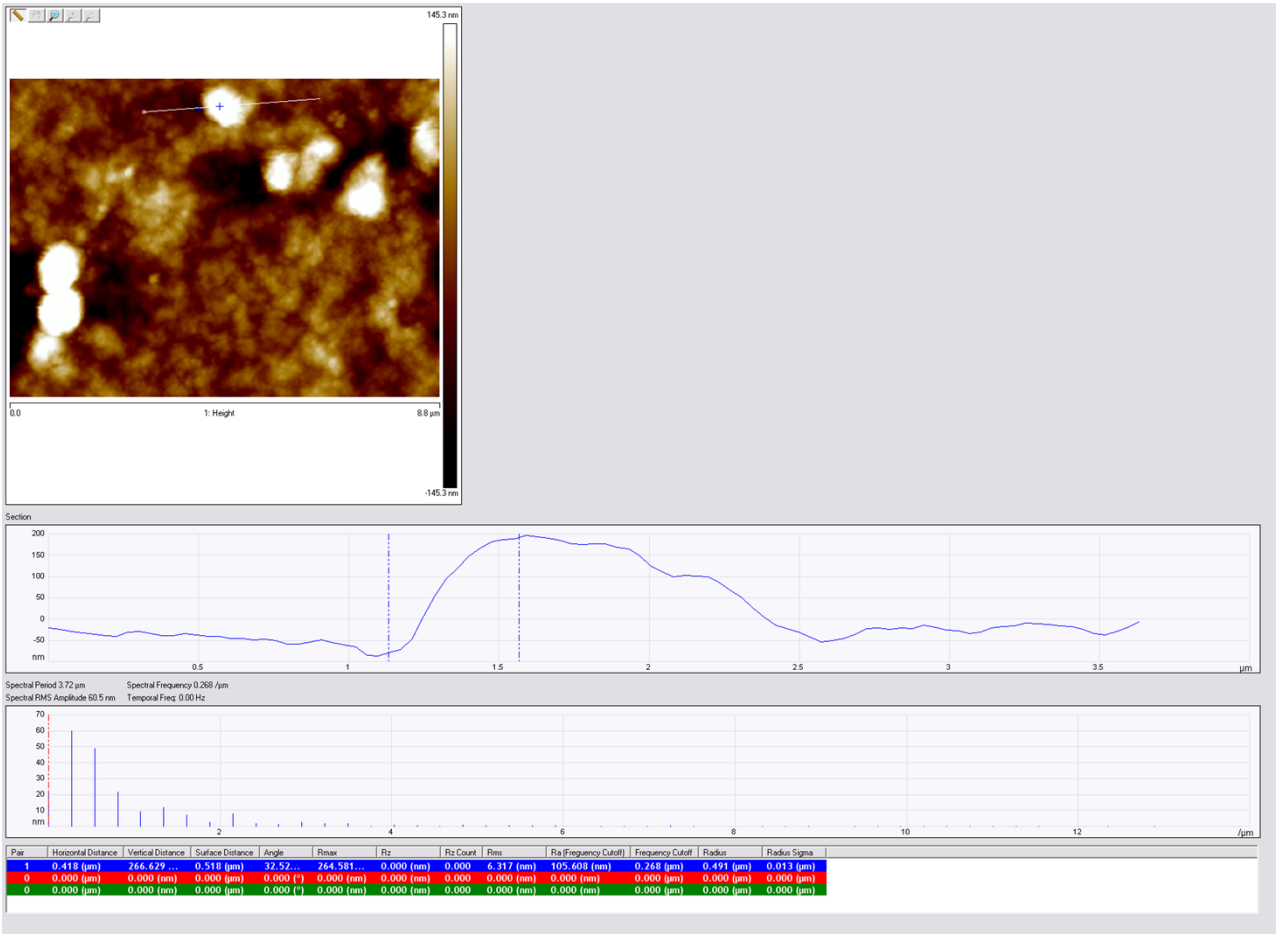

Fig. S13. AFM results of the polymeric vesicles.

9. Loading of the drugs

Gefitinib was used as a hydrophobic model compound to be put into the polymeric micelles solution with a concentration of 1.00×10^{-5} M; then the suspension was sonicated for 30 min at room temperature. The unencapsulated hydrophobic gefitinib was removed by filtration.

Gemcitabine was used as a hydrophilic model compound to be put into the polymeric vesicles solution with a concentration of 1.00×10^{-5} M. In order to remove the gemcitabine molecules outside the vesicles, dialysis was performed for 2 days until few calcein molecules were outside the vesicles before we measured the fluorescence change.

10. In vitro intracellular trafficking

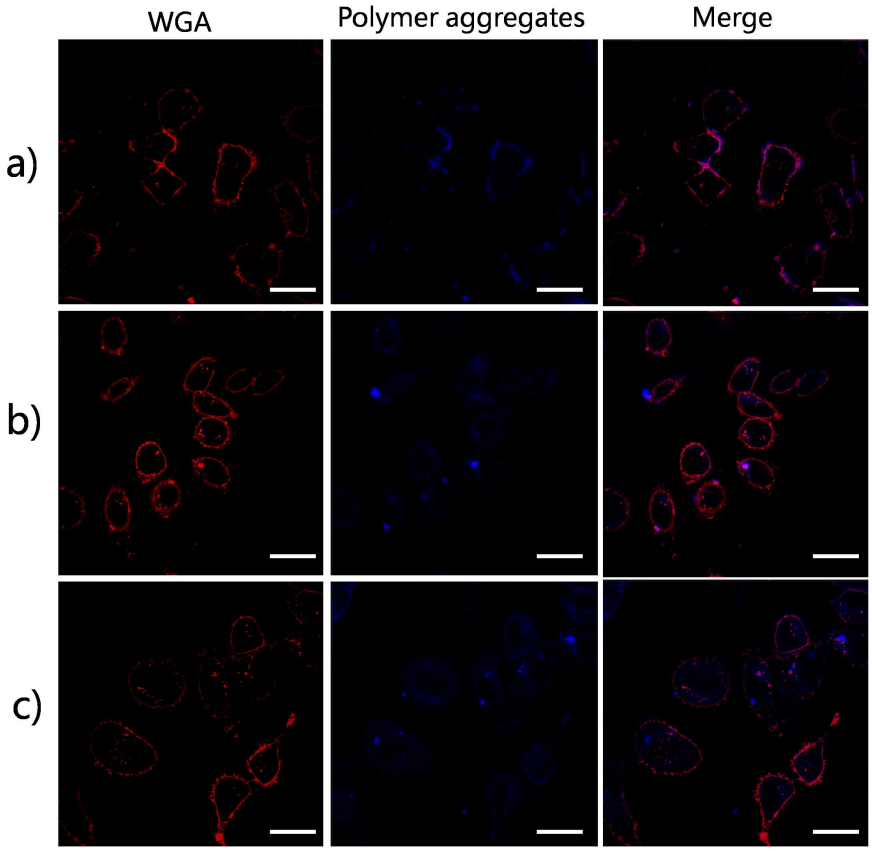

Fig. S14. Confocal laser scanning microscopic images of HepG2 cells incubated with (a) polymer **1**, (b) polymeric vesicles, and (c) polymeric micelles (scale bar denotes 20 μm).

The cellular internalization of the polymeric micelles and vesicles assembled from the supramolecular amphiphilic graft copolymers was examined against HepG2 cells as monitored by confocal laser scanning microscopy (CLSM; Fig. S14).[S5] The cell membranes were stained red by WGA. As shown in Figure 6a, after a 4 h incubation of the HepG2 cells with polymer **1**, some TPE moieties were found on the edge of the cell membranes. However, a small/large number of TPE moieties were found in the cell membranes for the polymer vesicles and micelles, respectively (Fig. S14b and Fig. S14c). The failure of polymer **1** to enter the cell membrane resulted from its very poor solubility in water. For the amphiphilic polymer vesicles and micelles, micelles displayed faster cellular uptake rate than vesicles because of their relatively smaller volume. Therefore, these fluorescent polymeric aggregates are candidates for delivery vehicles for intracellular delivery.

References:

S1. A. Natarajan, A. A. P. Burns, S. Jain and P. J. McCloskey, US 2013/0164531 Al, **2013**.

S2. X. Ji, J. Li, J. Chen, X. Chi, K. Zhu, X. Yan, M. Zhang and F. Huang, *Macromolecules,* 2012, **45**, 6457.

S3. Z.-Yi. Qiao, R. Ji, X.-N. Huang, F.-S. Du, R. Zhang, D.-H. Liang and Z.-C. Li, *Biomacromolecules,* 2013, **14**, 1555.

S4. L. N. Winslow, D. P. Rillema, J. H. Welch and P. Singh, *Inorg. Chem.,* 1989, **28**, 1596.

S5 J. Shen, Q. Wang, Q. Hu, Y. Li, G. Tang and P. K. Chu, *Biomaterials,* 2014, **35**, 8621.